# Structure dynamics of strongly reduced epitaxial $BaTiO_{3-x}$ studied by Raman Scattering

HZ Guo, ZH Chen *, BL Cheng, HB Lu, LF Liu, and YL Zhou

*Institute of Physics and Center for Condensed Matter Physics, Chinese Academy of Sciences, P.O. Box 603, Beijing 10008, China*

**Abstract:** Raman scattering technique was used to study structure dynamics of strongly reduced epitaxial barium titanate thin films grown on MgO (100) substrates by laser molecular beam epitaxy under different oxygen pressures from $10^{-2}$ Pa to $10^{-5}$ Pa. X-ray diffraction and asymmetric rocking curves indicate that lattice parameters *c* and *c*/*a* ratio increase, and *a* slightly decreases with decreasing oxygen pressure, indicating increased lattice volume of $BaTiO_{3-x}$ thin film. Raman spectra confirm that $BaTiO_{3-x}$ thin films are in tetragonal phase with some deviated features, which maybe origin from tensile strain at film-substrate interface due to lattice parameter mismatch. Moreover two weak peaks in Raman spectra of $BaTiO_{2.52}$ thin film grown under $3.0\times10^{-5}$ Pa may be induced by second-order two-phonon processes. Raman peaks shift towards lower frequency with decreasing oxygen pressure during deposition, suggesting a decreases of the stress in $BaTiO_{3-x}$ thin films. In the meantime, Raman peaks become broaden, which may be attributed to higher degree of structural disorder in strongly reduced $BaTiO_{3-x}$ lattice structure.

**Key words: Films; Defects; Spectroscopy; X-ray methods; Optical properties; $BaTiO_3$.**

## 1. INTRODUCTION

Recently, a number of studies have been focused on barium titanate ($BaTiO_3$) thin films due to their remarkable ferroelectric, electro-optical, high dielectric constant, and nonlinear optical properties.[1-4] To meet the need of advanced integrated electronic devices, $BaTiO_3$ films with small dimensions and perfect crystallinity and surface morphology are required.

* Corresponding author. Tel.: +86-10-82649478; fax: +86-10-82649451.

It has been found that the crystallinity and surface morphology of thin films can be improved by decreasing gas pressure during growth [5, 6]. Therefore, many efforts have been made to deposit $BaTiO_3$ films with small dimensions under low oxygen pressures. Unfortunately, it has also been revealed that dielectric and ferroelectric properties of thin films degrade with decreasing oxygen pressure due to generation of oxygen vacancies.[7] This means that oxygen deficient plays important roles in dielectric and ferroelectric performance. Hence, tracking the structural dynamic characteristics of $BaTiO_3$ films as a function of deposition oxygen pressure is very important.

On the other hand, stress caused by difference of lattice mismatch and thermal expansion coefficient between thin film and substrate has always been one of the major interests in the study of ferroelectric thin films. It has been found that stress can significantly change the mechanical, dielectric and optical properties, and influence the nature of phase transitions, and enhance the dielectric constant of $BaTiO_3$ greatly.[8] It is well known that Raman spectroscopy is a characterization method that measures the frequencies of the long-wavelength lattice vibrations (phonons). Unlike XRD or electron diffraction, Raman spectroscopy does not provide direct determination of the crystal structure, however, it has several advantages other than the diffraction methods as follows: Raman spectroscopy can give useful information about impurity, grain size, porosity and crystal symmetry of thin films.[9, 10] Furthermore, Raman scattering is greatly influenced by disorder and residual stress, which causes variation in phonon frequencies and life times, leading to broadening of Raman peaks and breakdown of Raman selection rule. The frequencies of phonons are sensitive to strains, i.e. Raman peaks shift towards higher (lower) frequency are related to compressive (tensile) strains.[11] In the last few years, a number of groups have studied the Raman spectra of BTO single crystals[10, 12-14] and ferroelectric single-domain crystal at

E-mail address: zhchen@aphy.iphy.ac.cn.

room- temperature[15,16]. However, Raman investigations of epitaxial BTO thin films are still rare in literature.

In this paper, $BaTiO_{3-x}$ thin films grown on single-crystal MgO (100) substrates by laser molecular-beam epitaxy (L-MBE)[17] under various oxygen pressures from $10^{-2}$ to $10^{-5}$ Pa are investigated using Raman spectroscopy in combination with X-ray diffraction (XRD), and Rutherford backscattering spectrometry (RBS). Raman spectroscopy has been demonstrated as a powerful tool to study the structural dynamics based on effects of the oxygen deficient and stress in ferroelectric thin films.

## 2. EXPERIMENTS

$BaTiO_{3-x}$ thin films were prepared on MgO (100) substrates by L-MBE using $BaTiO_3$ single-crystal target. Distance from target-to-substrate was 4.5 cm. During deposition the substrate temperature was kept at 630 $^oC$ with different oxygen pressures of $3\times10^{-2}$, $3\times10^{-3}$, $3\times10^{-4}$, and $3\times10^{-5}$ Pa, respectively. A Lambda Physik LEXTRA 200 excimer laser (308 nm, 28 ns) was used as the deposition light source with an energy density of about 1 J/cm$^2$ at a repetition rate of 2 Hz. The deposition rate was about 0.1 nm/pulse. *In situ* reflection high-energy electron diffraction (RHEED) was used to characterize the growth process of the $BaTiO_{3-x}$ thin films. The thickness of the $BaTiO_{3-x}$ thin films was about 300 nm.

The crystallinity and phase purity of the $BaTiO_{3-x}$ thin films were examined by XRD with Cu $K\alpha$ radiation. The oxygen pressure dependence on the crystallographic orientation and crystal parameters of $BaTiO_{3-x}$ thin films were investigated using asymmetric rocking curve method.[18-20] Oxygen content in the thin films was measured by RBS with an incident $^4He^+$ (3.016 MeV in energy) ion beam, which is effective to detect oxygen.[21] Raman scattering measurements were carried out at room temperature in backscattering geometry with a Jobin-Yvon T64000 triple Raman spectrometer. A 514.5 nm $Ar^+$ ion laser line was used for excitation. Raman spectra were obtained using a microprobe device that allows the incident light to be focused on the sample with about 1~2 μm in diameter. The spectrometer provided a wave number resolution of ~0.5 $cm^{-1}$ and accuracy of ~0.1 $cm^{-1}$.

## 3. RESULTS AND DISCUSSION

### 3.1. RHEED, XRD, and RBS results

A typical RHEED pattern during epitaxial growth of the $BaTiO_{3-x}$ (BTO) thin film under $3.0\times10^{-5}$ Pa oxygen pressure is shown in Fig. 1. RHEED pattern indicates that the BTO thin films have high crystallinity. The thickness of the BTO thin films was *in situ* controlled at atomic scale by monitoring of the intensity oscillation of RHEED.

A typical XRD $\theta$-$2\theta$ pattern of a 300-nm-thick BTO thin film grown under $3\times10^{-5}$ Pa oxygen pressure on MgO substrate is shown in Fig.2. Only (00*l*) diffraction peaks of BTO and (*l*00) diffraction peaks of MgO can be observed, which means that the deposited BTO thin films are single phase. The quite narrow XRD $\omega$-rocking curves on (002) BTO, as shown by inset in Fig. 2, reveal that the BTO films are well-oriented. The full width at half-maximum (FWHM) is 0.82° for the (002) peak indicating that the films have a high degree of crystallinity. To study the relationship between the crystal structure and oxygen pressures, the asymmetric rocking curve technique is taken for the {303} family of the equivalent planes in two perpendicular directions rotated 90° about the surface normal. By using XRD $\theta$-$2\theta$ and asymmetric $\omega$ rocking curve, the phase and orientation of the $BaTiO_{3-x}$ films are identified to be tetragonal with *c*-axis orientation.

Variations of parameters *c*, *a* and *c*/*a* ratio as a function of oxygen pressure are plotted in Fig. 3. The open square, open circle and solid triangle represent the experimental data and the solid lines are guides to eye. As the oxygen pressure decreases, *c* and *c*/*a* increase while *a* slightly decreases, indicating that the lattice volume of the $BaTiO_{3-x}$ thin film increases under lower oxygen pressure. This increase of lattice volume can be attributed to the effect of oxygen vacancies.[19, 22] According to the investigation on $PbTiO_3$[22], oxygen vacancies are double donor defects. The nearest two $Ti^{4+}$ and four $Pb^{2+}$ cations of a +2 charged oxygen vacancy are displaced away from it, while the nearest eight $O^{-2}$ anions are attracted towards it. The displacements of $Ti^{4+}$ and $Pb^{2+}$ cations are along *c* axis and *a* axis, respectively. The magnitude of the displacements from ideal tetragonal positions of Ti, O, and Pb atoms are 0.021, 0.004, and 0.016 nm, respectively. Resulting from these displacements, the unit cell volume and the c/a ratio of $PbTiO_3$ are enlarged as the oxygen pressure decrease. It is reasonable to deduce that the effect of the oxygen vacancies on the lattice structure of $BaTiO_3$ is similar to that of $PbTiO_3$, because $BaTiO_3$ and $PbTiO_3$ belong to the same perovskite structure.

Furthermore, in order to find out how the structure of BTO thin films grown under different oxygen being different, the oxygen content in BTO thin films grown under different oxygen was analyzed by RBS as shown in Table 1. It can be seen that the stoichiometric BTO thin film is obtained for the sample deposited under $3.0\times10^{-2}$ Pa. As the oxygen pressure decreases, the oxygen deficiency increases. When deposited under $3.0\times10^{-5}$ Pa, the oxygen deficiency in BTO film is 0.48. Our results clearly show that more oxygen vacancies exist in the film grown under the oxygen pressure of $3.0\times10^{-5}$ Pa. The results also indicate that tetragonal perovskite structure can be maintained even in the strongly reduced $BaTiO_{0.52}$ sample, which may be due to the stabilization of the tetragonality even though the large misfit tensile stress in $BaTiO_{3-x}$ thin films.

**3.2. Raman mode assignments and analyses**

Single-crystal $BaTiO_3$ has a tetragonal structure at room temperature and has a tetragonal-cubic phase transition at its Curie temperature ($T_c$=132 °C). In the cubic phase, the 12 optic modes transform as the $3F_{1u}+1F_{2u}$ irreducible representations, and there are no first-order Raman active modes. In the tetragonal phase, each $F_{1u}$ mode splits into one $A_1$ mode and one E mode, while the $F_{2u}$ mode splits into $B_1$ and E, resulting in $3A_1+B_1+4E$ modes. These modes further split into longitudinal (LO) and transverse (TO) components due to the long range electrostatic forces associated with lattice ionicity. Then the following distinct Raman-active optical lattice vibrations for BTO in its tetragonal phase are obtained: $A_1(TO)+3A_1(LO)+3E(TO)+3E(LO)+1E(LO+TO)+1B_1$.[12] The Raman[10-16, 23] and infrared spectral[24] modes have been reliably identified in BTO bulk crystal in the ferroelectric single and poly domain states. These results mentioned above will be used in the following section to compare with our results on the epitaxial film.

Figs. 4 (I)-(II) show the Raman spectra of the 300-nm-thick $BaTiO_{3-x}$ thin films on MgO substrates grown under different oxygen pressure. The centrosymmetric structure of the cubic forbids any first order Raman scattering process. Thus, the optical phonons in bulk MgO are Raman inactive due to cubic symmetry of MgO.[25] Therefore, Raman scattering from the MgO substrate can be avoided and the signal from BTO film can be confidently detected. Spectra are also re-scaled and offset for ease of comparison. Let us examine the features of the spectra in Fig. 4 (I) in the order of increasing wave number. First, the interference of the $A_1(TO_1)$ mode at about ~185 $cm^{-1}$ with a broad $A_1(TO_2)$ mode about 280 $cm^{-1}$, which is due to the coupling between $A_1$ modes, results in an antiresonance effect at 180 $cm^{-1}$. Several investigators have studied this coupling phenomenon of $A_1$ modes in $BaTiO_3$.[14] Next is the third asymmetric $A_1(TO_3)$ modes at about ~532 $cm^{-1}$ that also couples weakly with the $A_1(TO_2)$ mode. The $E(TO_2)$ mode at 305 $cm^{-1}$ mixing with the broad bands $A_1(TO_2)$ mode and the high frequency at ~742 $cm^{-1}$ ($A_1(LO_3)$) are observed, which are specific to the tetragonal phase of BTO.[10, 11] Thus the Raman spectra confirm that the BTO thin films have the tetragonal structure in agreement with the XRD results, which confirmed that the samples are *c*-axis orientation of tetragonal phase. Finally, two weak peaks at 832 and 877 $cm^{-1}$ marked with a single asterisk in Fig. 4 maybe origin from the tensile strain at the film-substrate interface due to the lattice parameters mismatch between the BTO single crystal and MgO (100) substrate, which were not observed by XRD measurements. Another interesting feature is the occurrence of two weak peaks at 943 and 1039 $cm^{-1}$ marked with the double asterisks, which is only observed in the spectrum of $BaTiO_{2.52}$ thin film grown under $3.0\times10^{-5}$ Pa. These two peaks are broad and weak, which seem to be related to the second-order two-phonon processes.[26] Oxygen deficiency makes the $BaTiO_{3-x}$ lattice distorted, the more oxygen deficiency, the more the $BaTiO_{3-x}$ lattice distorted would be. Because of the loss of translation symmetry in the $BaTiO_{0.52}$ due to the distortion of the lattice, the phonons are not restricted to originate from a point near the Brillouin zone center. So that the phonons can originate anywhere in the Brillouin zone provided their wave vectors add up to approximately zero. This maybe account for the second-order two-phonon processes in the strongly reduced $BaTiO_{0.52}$ thin film.

It can be observed from Figs. 4 (I) and (II) that all the Raman modes observed in these $BaTiO_{3-x}$ thin films are found at higher frequencies (blue shift) than the corresponding modes in BTO single crystal.[10, 12-14] Moreover, the Raman spectra also show that the blue shifts of the Raman modes become smaller and smaller with decreasing oxygen pressure. Meanwhile, Raman scattering results, displayed in Figs. 4(I) and (II), show that the peaks decrease in intensity with decreasing oxygen pressure during deposition, and the bands broaden more and more. We used Lorentzian functions to fit the $A_1(TO_3)$ and $A_1(LO_3)$ peaks. The corresponding results of the Raman shift and peak width as a function of the oxygen pressure are plotted in Figs. 5. It is found that the $A_1(TO_3)$ and $A_1(LO_3)$ peaks shift to lower frequency, but the peak width increases continuously with decreasing oxygen pressure.

The observed broadening of the Raman peaks maybe arises from the coupling of the normal modes with the static distortion.[27] The distortion of the lattice leads to the breakdown of the translation symmetry, thus the **q**=0 Raman selection rules are relaxed. The phonon frequencies also shift remarkably towards higher/lower value; depending upon the tensile/compressive nature of the stresses.[11] The blue shifts of the Raman modes are the characteristic of the presence of the tensile stresses in our samples. Chen *et.al* [28] have also found the presence of the tensile stresses in the Ce doped BTO thin films on MgO substrates. Furthermore, the Grüneisen law: $\Delta\nu/\nu = -\gamma\Delta V/V$, provides a good approximation for the frequency shift due to lattice enlarged.[29] At lower oxygen pressure, the density of oxygen vacancies is higher, and then the expansion of the lattice volume is greater. Then the Raman modes shift to lower frequencies (see Fig. 4). Meanwhile, the lattice mismatch between $BaTiO_{3-x}$ thin films and MgO substrate becomes smaller, indicating the releasing of the residual stresses occurred through oxygen vacancies generation. Moreover, oxygen deficiency makes the $BaTiO_{3-x}$ lattice distorted, which further make the broadening of the peaks and appearances of new Raman peaks.

## 4. CONCLUSION

In conclusion, a series of highly *c*-axis oriented strongly reduced epitaxial $BaTiO_{3-x}$ thin films were epitaxially grown with different oxygen pressures from $3.0\times10^{-2}$ to $3.0\times10^{-5}$ Pa on MgO by L-MBE. A relationship between the structural parameters and the density of oxygen vacancies of the samples were systematically investigated. The results indicate that, with a decrease of oxygen pressure during deposition, the oxygen deficiency and the cell volume increase increases, while the perovskite structure can be maintained in strongly reduced $BaTiO_{3-x}$ with the oxygen deficiency being as high as 0.48. Furthermore, the structure dynamics in the samples, such as stress effect, oxygen defects, structural disorder, *ect.* depending on oxygen deficiency have been investigated by means of Raman scattering.

The results indicate that, with a decrease of oxygen pressure during deposition, the stress in $BaTiO_{3-x}$ thin films becomes smaller; in the meantime the structural disorder becomes larger. In addition, two weak peaks at 943 and 1039 $cm^{-1}$ in strongly reduced $BaTiO_{2.52}$ thin film seem to be related to the second-order two-phonon processes.

**ACKNOWLEDGMENT**

The authors would like to thank Yulong Liu and Ke Zhu for their helps in Raman scattering measurements and for many fruitful discussions. The work was financially supported by the National Natural Science Foundation of China.

## Reference

[1] Sayer, M. & Sreenivas, K., Ceramic thin films: fabrication and applications. Science 1990, **247**, 1056-1060.

[2] Cohen, R. E, Origin of ferroelectricity in perovskite oxides. Nature, 1992, **358**, 136-138.

[3] Lee, M. B., Kawasaki, M., Yoshimoto, M. &Koinuma, H., Heteroepitaxial growth of $BaTiO_3$ films on Si by pulsed laser deposition. Appl. Phys. Lett., 1995, **66**, 1331-1333.

[4] Roy, D. & and Krupanidhi, S. B., Pulsed excimer laser ablated barium titanate thin films. Appl. Phys. Lett., 1992, **61**, 2057-2059.

[5] Shigetani, H., Kobayashi, K., Fujimoto, M., Sugimura, W., Matsui. Y. &Tanaka, J., $BaTiO_3$ thin films grown on $SrTiO_3$ substrates by a molecular-beam-epitaxy method using oxygen radicals. J. Appl. Phys., 1997, **81**, 693-697.

[6] Yoneda, Y., Okabe, T., Sakaue, K., Terauchi, H., Kasatani, H. &Deguchi, K., Structural characterization of $BaTiO_3$ thin films grown by molecular beam epitaxy. J. Appl. Phys., 1998, **83**, 2458-2461.

[7] Fukuda, Y., Haneda, H., Sakaguchi, I., Nuwata, K., Aoki, K. &Nishimura, A., Dielectric

Properties of (Ba, Sr)$TiO_3$ Thin Films and their Correlation with Oxygen Vacancy Density. Jpn. J. Appl. Phys., 1997, Part 2 **36**, L1514-L1516.

[8] Yano, Y., Iijima, K., Daitoh, Y., Terashima, T., Bando, Y., Watanabe, Y., Kasatani, H. & Terauchi, H., Epitaxial growth and dielectric properties of $BaTiO_3$ films on Pt electrodes by reactive evaporation. J. Appl. Phys., 1994, **76**, 7833-7838.

[9] Siu, G. G., Stokes, M. J. & Liu, Y. L., Variation of fundamental and higher-order Raman spectra of $ZrO_2$ nanograins with annealing temperature. Phys. Rev. B, 1999, **59**, 3173-3179.

[10] Robins, L. H., Kaiser, D., Rotter, L. D., Schenck, P. K., Stauf, G. T. & Rytz, D., Investigation of the structure of barium titanate thin films by Raman spectroscopy. J. Appl. Phys., 1994, **76**, 7487-7498.

[11] Wickboldt, P., Anastassakis, E., Sauer, R. & Cardona, M., Raman phonon piezospectroscopy in GaAs: Infrared measurements. Phys. Rev. B, 1987, **35**, 1362-1368.

[12] DiDominco, M., Wemple, S. H., Porto, S. P. S. & Bauman, R. P., Raman Spectrum of Single-Domain $BaTiO_3$. Phys. Rev., 1968, **174**, 522-530.

[13] Wang, R. P., Jiang, Y. J., Zeng, L. Z., Liu, Y. L. & Zhu, Y., Dispersion of the oblique phonons in tetragonal $BaTiO_3$ and Ce:$BaTiO_3$. J. Raman. Spectrosc., 1995, **26**, 295-299.

[14] Chaves, A., Katiyar, R. S. & Porto, S. P. S., Coupled modes with $A_1$ symmetry in tetragonal $BaTiO_3$. Phys. Rev. B, 1974, **10**, 3522-3533.

[15] Tarrach, G., Lagos L., P. & Hermans Z., R., Nanometer spot allocation for Raman spectroscopy on ferroelectrics by polarization and piezoresponse force microscopy. Appl. Phys. Lett., 2001, **79**, 3152-3154.

[16] Jiang, Y. J., Zeng, L. Z., Wang, R. P., Zhu, Y. & Liu, Y. L., Fundamental and second-order Raman spectra of $BaTiO_3$. J. Raman. Spectrosc, 1996, **27**, 31-34.

[17] Cui, D. F., Lu, H. B., Wang, H. S., Chen, Z. H., Zhou, Y. L., Yang, G. Z. Yang, H. T. Tao, H. J. & Li. L., Atomic force microscopy studies of barium titanate thin films prepared by

laser molecular beam epitaxy. Chin. Phys. Lett., 1997, **14**, 134-137.

[18] Li, C. L., Cui, D. F., Zhou, Y. L., Lu, H. B., Chen, Z. H., Zhang, D. F. & Wu, F., Asymmetric rocking curve study of the crystal structure orientations for $BaTiO_3$ thin films grown by pulsed laser deposition. Appl. Surf. Sci. 1998, **136**, 173-177.

[19] Zhao, T., Chen, F., Lu, H. B., Yang, G. Z. & Chen, Z. H., Thickness and oxygen pressure dependent structural characteristics of $BaTiO_3$ thin films grown by laser molecular beam epitaxy. J. Appl. Phys. 2000, **87**, 7442-7447.

[20] Kang, M. H., Ku, J. K., & Baik, S., Crystallographic characterization of tetragonal $(Pb,La)TiO_3$ epitaxial thin films grown by pulsed laser deposition. J. Appl. Phys., 1995, **78**, 2601-2606.

[21] Cheng, H. S., Shen, H., Tang, J. Y. &Yang, F. J., Cross sections for 170° backscattering of $^4He$ from oxygen in the energy range of 2.0–9.0 MeV. Nucl. Instrum. Methods. Phys. Res. B, 1993, **83**, 449-453.

[22] Park, C. H. & Chadi, D. J., Microscopic study of oxygen-vacancy defects in ferroelectric perovskites. Phys. Rev. B, 1998, **57**, R13961-R13964.

[23] Kim, T. W., Jung, M. & Kim, H. J., Structural and electrical properties of $BaTiO_3$ thin films grown on *p*-InSb substrate by metalorganic chemical vapor deposition at low temperature. Appl. Phys. Lett. 1994, **62**, 1788-1790.

[24] Sanjurjo, J. A., Katiyar, R. S. & Porto, S. P. S., Temperature dependence of dipolar modes in ferroelectric $BaTiO_3$ by infrared studies. Phys. Rev. B, 1980, **22**, 2396-2403.

[25] Yuzyuk, Y. E., Alyoshin, V. A., Zakharchenko, I. N., Sviridov, E. V., Almeida, A. & Chaves, M. R., Polarization-dependent Raman spectra of heteroepitaxial $(Ba,Sr)TiO_3/MgO$ thin films. Phys. Rev. B **65**, 134107 (2002).

[26] Hayes, W. & Loudon, R. Scattering of light by crystals.John Wiley ans sons, New York, 1978, pp. 121-131.

[27] Uwe, H., Lyons, K. B., Carter, H. L. & Fleury, P. A., Ferroelectric microregions and Raman scattering in $KTaO_3$. Phys. Rev. B, 1986, **33**, 6436.

[28] Chen, M. S., Shen, Z. X., Tang, S. H., Shi, W. S., Cui, D. F. & Chen, Z. H., Stress effect on Raman spectra of Ce-doped $BaTiO_3$ films. J .Phys.: Condens. Matter., 2000, **12** 7013-7023.

[29] Granado, E., Garcia, A., Sanjurjo, J. A., Rettori, C., Torriani, I., Prado, F., Sanchez, R. D., Caneiro, A. & Oseroff, S. B., Magnetic ordering effects in the Raman spectra of $La_{1-x}Mn_{1-x}O_3$. Phys. Rev. B, 1999, **60**, 11879-11882.

## Table CAPTIONS

Table 1. The chemical composition data of the $BaTiO_{3-x}$ thin films prepared under various oxygen pressures from RBS measurements.

| Oxygen Pressure (Pa) | Chemical Composition | | | Oxygen deficiency | Thickness (nm) |
|---|---|---|---|---|---|
| | Ba | Ti | O | x | |
| $3.0\times10^{-2}$ | 0.96 | 1.00 | 3.00 | 0 | 300 |
| $3.0\times10^{-3}$ | 0.96 | 1.00 | 2.93 | 0.07 | 300 |
| $3.0\times10^{-4}$ | 0.94 | 1.00 | 2.82 | 0.18 | 300 |
| $3.0\times10^{-5}$ | 0.94 | 1.01 | 2.52 | 0.48 | 300 |

Table 1.

FFIGURE CAPTIONS

Fig. 1. Typical RHEED pattern during the epitaxial growth of the $BaTiO_{3-x}$ thin film substrate at 670 $^{o}$C under $3.0\times10^{-5}$ Pa oxygen pressure.

Fig. 2. XRD $\theta$-$2\theta$ scan of 300-nm-thick $BaTiO_{3-x}$ thin films grown under $3.0\times10^{-5}$ Pa oxygen pressure on MgO substrate. The inset shows the $\omega$ rocking curve for the (002) peak of $BaTiO_{3-x}$ thin films.

Fig. 3. Lattice parameters *c*, *a,* and *c*/*a* ratio of $BaTiO_{3-x}$ thin films vs. oxygen pressure.

Fig. 4 (I) Raman spectra of 300-nm-thick $BaTiO_{3-x}$ thin films on MgO substrates. $BaTiO_{3-x}$ thin films were deposited under different oxygen pressures of (a) $3.0\times10^{-2}$ Pa, (b) $3.0\times10^{-3}$ Pa, (c) $3.0\times10^{-4}$ Pa and (d) $3.0\times10^{-5}$ Pa. Spectrum of a (100) oriented MgO substrate is also plotted here. (II) Raman spectra expanded scale.

Fig. 5. Oxygen pressure dependences of Raman shift and peak width for the $A_1(TO_3)$ and $A_1(LO_3)$ modes.

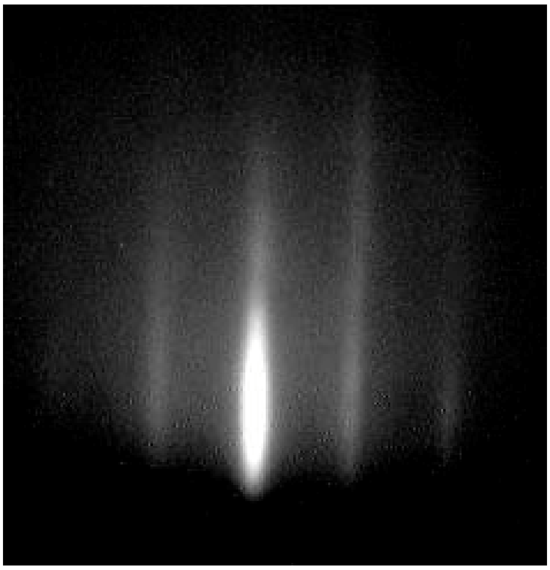

Figure 1

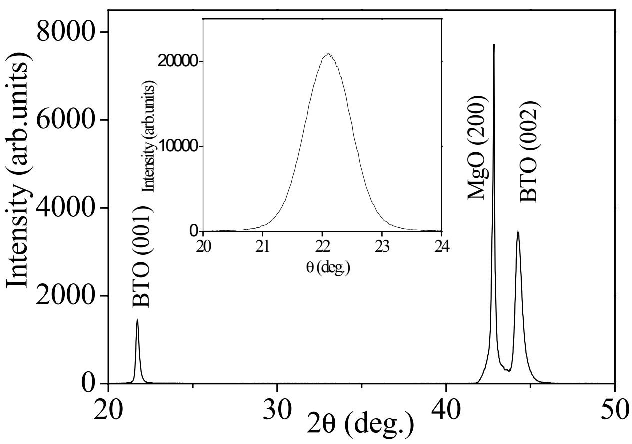


Figure 2

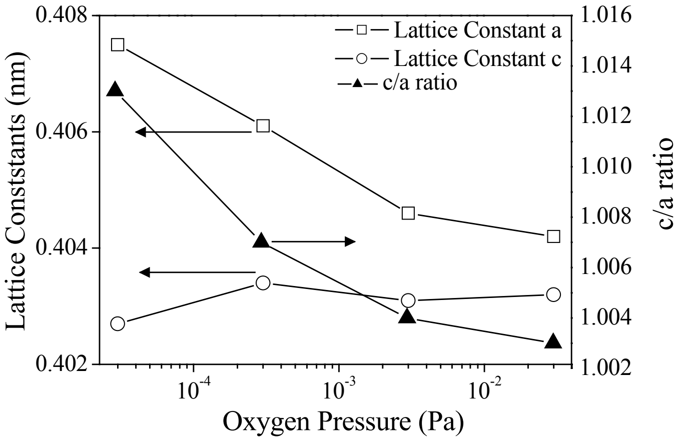

Lattice Constant a
Lattice Constant c
c/a ratio
0.408
0.406
0.404
0.402
1.016
1.014
1.012
1.010
1.008
1.006
1.004
1.002
Lattice Conststants (nm)
c/a ratio
$10^{-4}$
$10^{-3}$
$10^{-2}$
Oxygen Pressure (Pa)


Figure 3

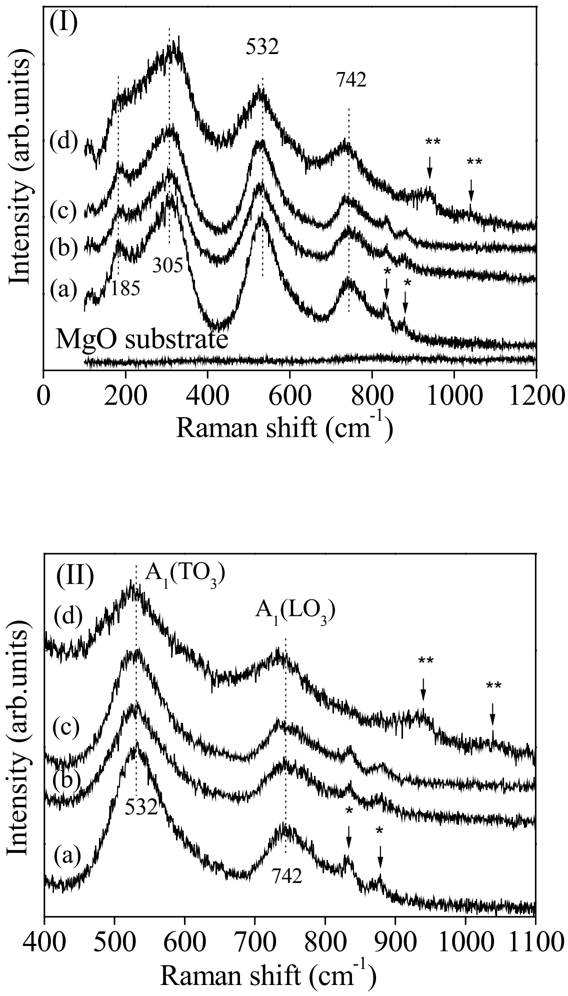

(I)
532
742
(d)
**
**
(c)
(b)
305
(a)
185
*
*
MgO substrate
Intensity (arb.units)
0 200 400 600 800 1000 1200
Raman shift (cm-1)
(II)
A1(TO3)
(d)
A1(LO3)
**
**
(c)
(b)
532
(a)
742
*
*
Intensity (arb.units)
400 500 600 700 800 900 1000 1100
Raman shift (cm-1)


Figure 4.

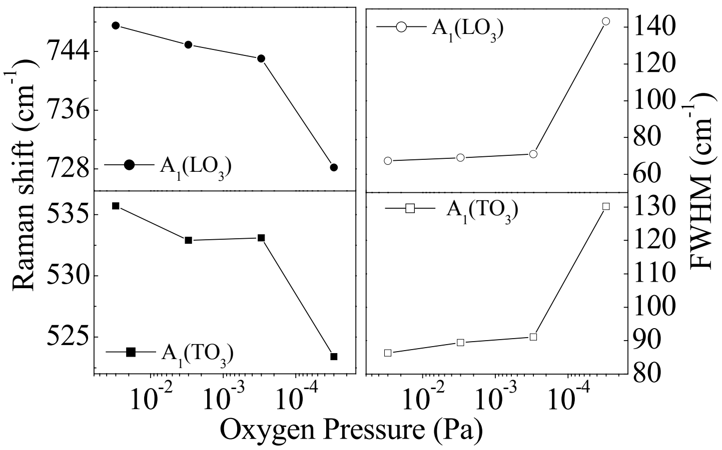
Raman shift (cm-1)
744
736
728
A1(LO3)
535
530
525
A1(TO3)
140
120
100
80
60
A1(LO3)
130
120
110
100
90
80
A1(TO3)
FWHM (cm-1)
10-2
10-3
10-4
10-2
10-3
10-4
Oxygen Pressure (Pa)

Figure 5